

LOW TEMPERATURE SOL-GEL SYNTHESIS OF TIN OXIDE NANOPARTICLES FOR PHOTOELECTROCHEMICAL SOLAR CELL APPLICATION

SAMBHAJI S. BHANDE

Department of Physic, baburaoji Adaskar Mahavidhyalaya, Kaij Dist Beed, Maharashtra, India. Email: sambhajibhande@gmail.com

Received: 25 January 2020, Revised and Accepted: 17 March 2020

ABSTRACT

A renewable energy has been always a topic of interest for researchers. The advances in solar cells from first generation to third generation solar cells have seen many materials. The low cost gratzel cells have made an impact on the solar cell manufacturing although the low efficiency as compared to silicon solar cells the low cost manufacturing and abundant material availability for large production makes it a potential candidate. The tin chloride precursor initiated sol-gel chemical method for synthesizing tin oxide (SnO_2) nanoparticles electrode is envisaged in dye-sensitized solar cells. Three steps; synthesis of nanoparticles, formation of paste using suitable surfactants and film development using doctor-blade method, are adopted for obtaining SnO_2 electrode. The films of SnO_2 nanoparticles formed onto glass and indium-tin-oxide substrates are annealed at 450 °C for 3 h. Influence of indium-tin-oxide on the structural elucidation, morphological evaluation, grain size confirmation and Raman shift analysis of the SnO_2 nanoparticles is eliminated by considering glass as the depositing substrate. Enhanced light absorbance at 500 nm due to the N719 dye molecules adsorption compared to pristine SnO_2 electrode has showed 1.62% solar-to-electrical conversion efficiency.

Keywords: Cobalt ferrite, Rare earth, Structural properties.

INTRODUCTION

Since the achievement of a solar to electrical energy conversion efficiency of over 11% achieved using a nanocrystalline TiO_2 electrode [1], large band gap semiconducting materials are enormously under investigation for their possible applications in dye-sensitized solar cells (DSSCs). The large band gap materials include TiO_2 , SnO_2 , WO_3 , MgO , ZnO , Nb_2O_5 , etc. [2, 3].

The tin oxide (SnO_2) is a chronic candidate when these semiconducting metal oxides are considered. Large surface area SnO_2 has many advantages including a faster rate of electron interception by the redox electrolyte, higher electronic mobility, low sensitivity to UV degradation due to its larger band gap and hence the better long-term stability [4], etc. Moreover, the lower conduction band edge (more positively located) position of SnO_2 facilitates the high efficiency of electron injections from the adsorbed dye molecules [5]. Along with these interesting properties several applications such as good adhesion to many polycrystalline and amorphous substrates including glasses, metals and oxides for the use of polycrystalline SnO_2 as transparent electrodes and thin film solid state gas sensor for different gases with high sensitivity, photovoltaic devices, transparent conductive films for display and solar cells, catalysis, and anode materials of secondary lithium ion battery etc., of SnO_2 have been numerous documented in the literature [6-11]. Several chemical and physical methods including chemical vapor deposition, chemical bath deposition, electrodeposition, high temperature thermal deposition, molten salt synthesis, laser ablation, dc and rf -sputtering etc. for synthesizing SnO_2 nanostructures including nanoparticles, nanoribbons, nanorods, nanowires and nanotubes etc. [11-15] are preferred as on today [16-21]. Implication of SnO_2 nanoparticles in DSSCs is limited by its open circuit voltage (V_{oc}), less than 400 mV [22] making it less attractive compared to TiO_2 and ZnO semiconductors. Conventional nanoparticles of SnO_2 have produced comparatively small conversion efficiencies of around 1-2% because of the inherent low conduction band edge and the fast recombination process [23].

In the present study, porous SnO_2 nanoparticles were procured from a simple, cost effective and low temperature sol-gel method. Two

substrates viz. glass and ITO were preferred for avoiding confusion of results between SnO_2 nanoparticles film and ITO substrate. To avoid

ITO substrate contamination the film of SnO_2 nanoparticles onto glass substrate was preferred for structural elucidation, morphological evolution and Raman shift analysis. For grain-size identification SnO_2 powder was scratched from the glass substrate and then mounted on the copper grid using fine-tipped syringe with acetone as a solvent. Change in absorbance, due to N719 dye molecules loading, was confirmed from an optical absorbance studies. The elemental chemical analysis was carried out from the energy dispersive X-ray (EDX) analysis. Prior to DSSCs use, the SnO_2 electrode was dipped in N719 dye for 3 h followed by acetonitrile rinsing. The current density-applied voltage (J - V) measurement of SnO_2 electrode of about two micrometer thickness and 0.25 cm^2 area was employed using 100 mW/cm^2 light intensity which was controlled with Si diode.

MATERIALS AND METHODS

Preparation of SnO_2 nanoparticles films onto glass and ITO substrates was divided into three parts; (a) synthesis of nanoparticles powder using sol-gel method, (b) formation of homogeneous paste followed by doctor blading scotch tape of two micron thickness, and (c) step-wise annealing in auto-controlled oven at 450 °C for 3 hr. All the chemicals were purchased from Sigma-Aldrich and used without further purification. For the synthesis of SnO_2 nanoparticles, initially 0.3 M tin tetrachloride (SnCl_4) was taken in ethanol solvent for 100 ml, after dissolving it, 0.6 M thioacetamide was further added to the same solution. The solution was then sealed in a falcon tubes of 100 ml with a magnetic sturrer inserted. The solgel deposition was carried out at 80 °C for 3 hrs. It must be noted that, if the time period exits above 3 hrs. the SnO_2 starts increase its particle size. The gel thus obtained were washed with ethanol and naturally dried in air and then annealed at 450 °C for 1 hr.

In second step, 0.5 gm crystalline SnO_2 nanoparticles powder was mixed with polyethylene glycol (0.5 ml), 0.5 ml 10wt% diluted acetyl acetone, one to two drops of triton X-100, 0.5 ml ethanol and 0.5 ml water while continuous stirring. Slurry was mixed well by continues

crushing in the mortar. The viscosity of the paste was controlled by ethanol and water followed by doctor-blading onto normal and ITO coated glass substrates using two micrometer thickness scotch tape. These prepared samples were annealed at 500 °C for 1 hr for crystallinity improvement. Prior to characterizations these samples were cooled naturally to room temperature.

RESULTS AND DISCUSSION

Figure 1 shows the XRD spectrum with intense and distinct peaks of SnO₂ nanoparticles film deposited onto glass substrate. Observed reflection peaks were compared with JCPDS (41-1445), and confirmed the presence of pure crystalline SnO₂. No peaks corresponding to tin metal or any other phase as impurity peaks were identified. The obtained peaks were with characteristic diffraction peaks of SnO₂ corresponding to (110), (101), (200), (111), (211), (220), (002), (310), (112), (301), (202), and (321) reflection planes. The grain size calculated from (110) peak was ~ 15 nm which later was confirmed from the high resolution transmission electron microscopy (HR-TEM) analysis fringes. Surface morphological evolution was confirmed from the SEM images recorded at different magnifications [Figure 1 b]. The identical SnO₂ spherical nanoparticles were seen in both photo-images. This morphology would be interesting for DSSCs due to its larger surface area and relatively smaller crystallite size. The calculated grain size of the SnO₂ nanoparticles was comparable to Debye length which can occupy the space charge region of SnO₂ completely by controlling its band structure [24]. Thus, the charge transportation should be easy which would reduce the charge recombination rate to great extent. The highly porous nature on its surface generally allows maximum dye adsorption for efficient solar-to-electricity conversion by maximum light harvesting. The EDX study of SnO₂ nanoparticles onto glass substrate was carried out for Sn and O elements. The wt.% ratio of Sn and O was 57:33, confirming the formation of stoichiometric SnO₂ using this method.

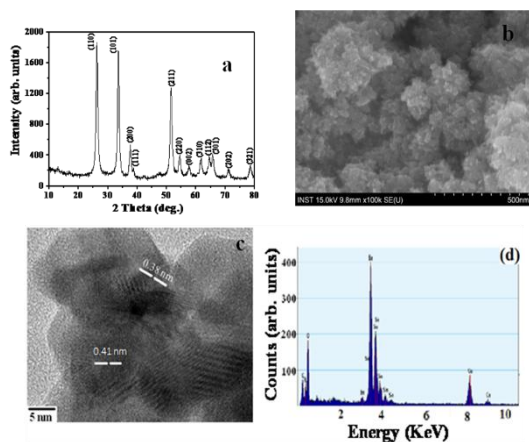


Fig.1.a) XRD pattern of SnO₂ b) SEM analysis c) TEM d) EDAX

In Figure 1 (c) HR-TEM images of SnO₂ nanoparticles are also presented. Spherical nanoparticles of SnO₂, consistent to the SEM images, were identical. Nearly 50 nanometer area was considered for obtaining the reflection fringes. Presence of spotted-lines instead of points or continuous lines has proved the nanostructure of SnO₂. The calculated inter planar 0.41 and 0.39 nm spacing's were closely matched to inter planar spacing's of (110) and (101) reflection planes (0.411 and 0.391 nm), respectively, of SnO₂. Unclear but uniform reflection circles are due to nanocrystalline form of SnO₂ as for amorphous metal oxides fuzzy pattern is dominant whereas, distinct regular spots are seen in crystalline metal oxides. The EDAX pattern (Figure 1-d) recorded while TEM analysis has confirmed existence of Sn and O in 56 and 34 wt% ratio.

The UV-visible absorbance spectrum was carried out in order to study optical behavior of the SnO₂ electrode as the quantum confinement effect is expected if the semiconductor dimensions become smaller than the Bohr radius of the exciton, and the absorbance edge will be shifted to the higher energy [25]. The

absorbance spectrum of pristine SnO₂ electrode and SnO₂ electrode after the dye loading was taken for the analysis. The absorbance edge in case of Pristine SnO₂ electrode is 515 nm where as the electrode with N719 dye loaded on its surface shows the absorbance edge at 655 nm and 695 nm, respectively (figure 2-a).

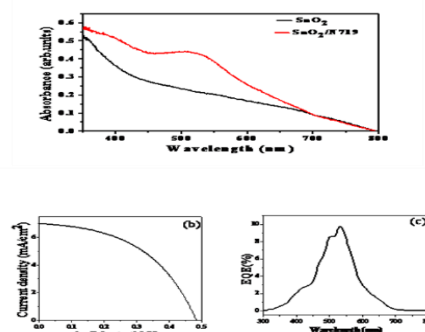


Fig.2: UV -Vis spectra b) JV curve c) IPCE curve

The *J-V* measurement of the SnO₂nanoparticles-N719 electrode, prepared by the sol-gel method, was tested for DSSCs application (Figure 2b). For the measurement, an electrolyte solution consisting of 15 mL iodide-tri-iodide solution was used. Obtained *V_{oc}* in the present case was superior to that of 150 mV reported earlier [26]. The uniformly distributed spherical SnO₂ nanoparticles could be responsible for 1.62% conversion efficiency, which is competitive to ZnO nanostructures [27, 28], one of the widely used metal oxides so far. The SnO₂ nanoparticles electrode with fill factor (*FF*=0.48), current density (*J_{sc}*=6.94), mA/cm², and (*V_{oc}*=0.47 V) was certainly inevitable. This is attributed to porous and nanocrystalline texture of SnO₂. High surface area and porous nature of SnO₂ nanoparticles must be responsible for efficient dye molecules absorbance followed moderate solar-to-electricity conversion efficiency. Contrary, in spite of high current density, IPCE (Figure 2c) value was close to 10, indicating that there was dominant recombination either at dye/electrolyte or conduction band of SnO₂ (-4.0 vs Normal hydrogen Electrode)/electrolyte interfaces. By surface engineering monitoring [29] or by using dyes of higher extinction coefficients [30, 31] SnO₂ nanoparticles device performance can be increased, which is underway.

CONCLUSION

Using sol-gel and doctor blade methods two micrometer thick SnO₂ nanoparticles electrodes were prepared onto glass and indium-tin-oxide substrates and explored for structural, optical and morphological properties and used in DSSCs application. The 57:33 stoichiometry, confirming the formation of SnO₂, for Sn and O elements was obtained from the EDX analysis. Phase confirmation was also carried out by X-ray diffraction. In spite of weak IPCE value, solar-to-electrical conversion efficiency of 1.66% was obtained due enhanced optical absorbance caused by N719 dye molecules adsorption onto SnO₂ nanoparticles. The IPCE value can be increased either by surface engineering monitoring or by using dyes of higher extinction coefficients, which is underway.

REFERENCES

1. Gratzel M., Conversion of sunlight to electric power by nanocrystalline dyesensitized solar cells. *J Photochem Photobiol A: Chem* 2004; 164,3-14.
2. Kuang, Je' re' mie Brillet D., Chen P., Takata, M. Uchida, S. Miura, H. Sumioka, K. Shaik, M.Z. Gratzel, M. Application of Highly Ordered TiO₂ Nanotube Arrays in Flexible Dye-Sensitized Solar Cells. *ACS nano* 2008;2: 1113-1116.
3. Zaban, A. Chen, S.G. Chappel, S. Gregg, B.A. Nanoporous Electrodes for Dye Sensitized Solar Cells. *Chem Commun* 2000;22: 2231- 2232.
4. Gubbala, S. Chakrapani, V. Kumar, V. Sunkara, M.K. Band-Edge Engineered Hybrid Structures for Dye-Sensitized Solar Cells Based on SnO₂ Nanowires. *Adv. Funct. Mater* 2008;18,

- :2411-2418.
5. Hara, K. Sato, T. Katoh, R. Furube, A. Ohga, Y. Shinpo, A. Suga, S. Sayama, K. Sugihara, H. Arakawa, H. Molecular Design of Coumarin Dyes for Efficient Dye-Sensitized Solar Cells. *J Phys Chem B* 2003;107:597-606.
 6. Li, Z. Wang, H. Liu, P. Zhao, B. Zhang Y. Synthesis and field-emission of aligned SnO₂ nanotubes arrays. *Appl Surf Sci* 2009;255: 4470-4473.
 7. Liu, Y. Liu, M. Growth of Aligned Square - Shaped SnO₂ Tube Arrays. *Adv Funct Mater* (2005);15: 57-62.
 8. Ma, Y.J. Zhou, F. Lu, L. Zhang, Z. Low-temperature transport properties of individual SnO₂ nanowires. *Solid State Commun.* 2004;130:313-316.
 9. Dai, Z.R. Pan, Z.W. Wang, Z.L. Ultra-long Single Crystalline Nanoribbon of Tin Oxide. *Solid State Commun* 2001;118:351-354.
 10. Dai, Z.R. Gole, J.L. Stout, J.D. Wang, Z.L. Tin Oxide Nanowires, Nanoribbons, and Nanotubes. *J Phys Chem B* 2002; 106:1274-1279.
 11. Jiang, X. Wang, Y. Herricks, T. Xia, Y. Ethylenediamine Glycol-Mediated Synthesis of Metal Oxide Nanowires. *Mater Chem* 2004;14: 695-703.
 12. Liu, Y. Zheng, C. Wang, W. Yin, C. Wang, G. Synthesis and Characterization of Rutile SnO₂ Nanorods. *Adv Mater* 2001;13:1883-1887.
 13. Dale, R.S. Rastomjee, C.S. Potter, F.H. Egdell, R.G. Sb and Bi implanted SnO₂ thin films: photoemission studies and application as gas sensors. *Appl Surf Sci* 1993;70/71: 359-362.
 14. Martel, A. Briones, F.C. Fandino, J. Rodriguez, R.C. Perez, P.B. Navarro, A.Z. Torres, M.Z. Pena, J.L. Chemical and phase composition of SnO_x:F films grown by DC reactive sputtering. *Surf Coat Technol* 1999;122:136-142.
 15. Thangadurai, P. Bose, A.C. Ramasamy, S. Kesavamoorthy, R. Ravindran, T.R. High Pressure effects on electrical resistivity and dielectric properties of nanocrystalline SnO₂. *J. Phys. and Chem. of Solids.* 2005; 66:1621-1627.
 16. Antonio, J.A.T. Baez, R.G. Sebastian, P.J. Vázquez, A.J. Thermal stability and structural deformation of rutile SnO₂ nanoparticles. *J. Solid State Chem* 2003;174: 241-248.
 17. Legendre, F. Poissonnet, S. Bonnailie, P. Synthesis of nanostructured SnO₂ materials by reactive ball-milling. *J Alloys Compd* 2007;434:400-404.
 18. Gu, F. Wang, S.F. Lü, M.K. Cheng, X.F. Liu, S.W. Zhou, G.J. Xu, D. Yuan, D.R. Luminescence of SnO₂ thin films prepared by spin-coating method. *J Cryst Growth* 2004;262: 182-185.
 19. Kim, W. Shim, S.H. Synthesis and characteristics of SnO₂ needle-shaped nanostructures. *J Alloys and Compd* 2006;426:286-289.
 20. Chappel, S. Zaban, A. Nanoporous SnO₂ electrodes for dye-sensitized solar cells: improved cell performance by the synthesis of 18 nm SnO₂ colloids. *Sol Energy Mater Sol Cells* 2002;71:141-152.
 21. Sayama, K. Sugihara, H. Arakawa. H. Photoelectrochemical properties of a porous Nb₂O₅ electrode sensitized by a ruthenium dye. *Chem Mater* 1998;10:3825-3832.
 22. Fukai, Y. Kondo, Y. Mori, S. Suzuki, E. Highly efficient dye-sensitized SnO₂ solar cells having sufficient electron diffusion length. *Electrochem Commun* 2007; 9: 1439-1443.
 23. Lee, J.H. Park, N.G. Shin, Y.J. Nano-grain SnO₂ electrodes for high conversion efficiency SnO₂-DSSC. *Sol Engy Mater sol Cells* 2011;95: 179-183.
 24. Yamazoe, N. New approaches for improving semiconductor gas sensors. *Sens Actuators B Chem* 1991;5:7-19.
 25. Kravets, V.G. Photoluminescence and Raman spectra of SnO_x nanostructures doped with Sm ions, *Opt Spectrosc* 2007;103:766-771.
 26. Gubbala, S. Chakrapani, V. Kumar, V. Sunkara, M.K. Band-edge engineered hybrid structures for dye-sensitized solar cells based on SnO₂ nanowires. *Adv Funct Mater* 2008;8:12411-2418.
 27. Kruk, M. Jaroniec, M. Gas adsorption characterization of ordered organic inorganic nanocomposite materials. *Chem Mater* 2001;13:3169-3183.
 28. Umar, A. Hajry, A.A. Hahn, Y.B. Kim, D.H. Rapid synthesis and dye sensitized solar cell applications of hexagonal-shaped ZnO nanorods. *Electrochimica Acta* 2009;54: 5358-5362.
 29. Prasittichai, C. Hupp, J.T. Surface modification of SnO₂ photoelectrodes in dye-sensitized solar cells: Significant improvements in photovoltage via Al₂O₃ atomic layer deposition. *J Phys Chem Lett* 2010;1: 1611-1615.
 30. Baraton, M. I. FTIR spectrometry as a quality control method for surface engineering of nanomaterials. *Mater Res Soc Proc* 2001;636:D811-D8110.
 31. Kuang, D. Klein, C. Ito, S. Moser, J.E. Baker, R.H. Zakeeruddin, S.M. Gratzel, M. High molar extinction coefficient Ion-coordinating Ruthenium sensitizer for efficient and stable mesoscopic dye sensitized solar cells. *Adv. Func. Mater.* 2007;17:154-160.